

THE CENTER SHIFT IN MÖSSBAUER SPECTRA OF MAGHEMITE AND ALUMINUM MAGHEMITES

G. M. DA COSTA,^{1,2} E. DE GRAVE,¹ L. H. BOWEN,³
R. E. VANDENBERGHE,¹ AND P. M. A. DE BAKKER¹

¹ Laboratory of Magnetism, Department of Subatomic and Radiation Physics
University of Gent, B-9000 Gent, Belgium

² On leave from Departamento de Química, Universidade Federal de Ouro Preto
Ouro Preto, MG, Brazil

³ Department of Chemistry, North Carolina State University
Raleigh, North Carolina 27695, USA

Abstract—Synthetic, relatively well-crystallized aluminum-substituted maghemite samples, γ -(Al_yFe_{1-y})₂O₃, with $y = 0, 0.032, 0.058, 0.084, 0.106$ and 0.151 have been studied by X-ray diffraction and zero-field Mössbauer spectroscopy in the range 8 K to 475 K, and also with an external field of 60 kOe at 4.2 K and 275 K. It was found that there are two different converging models for fitting the zero-field spectra of the maghemites with a superposition of two Lorentzian-shaped sextets, both resulting in inconsistent values for the hyperfine fields (H_{hf}) and/or the center shifts (δ) of the tetrahedral (A) and octahedral (B) ferric ions. From the applied-field measurements it is concluded that there is a constant difference of 0.12 ± 0.01 mm/s between δ_{B} and δ_{A} , regardless of the Al content. For the Al-free sample the center shifts are found as: $\delta_{\text{A}} = 0.370$ mm/s and $\delta_{\text{B}} = 0.491$ mm/s at 4.2 K and $\delta_{\text{A}} = 0.233$ mm/s and $\delta_{\text{B}} = 0.357$ mm/s at 275 K (relative to metallic iron), with an estimated error of 0.005 mm/s. Both δ_{A} and δ_{B} are observed to decrease with increasing Al concentration. The effective hyperfine fields for the non-substituted maghemite sample are: $H_{\text{eff,A}} = 575$ kOe and $H_{\text{eff,B}} = 471$ kOe at 4.2 K and $H_{\text{eff,A}} = 562$ kOe and $H_{\text{eff,B}} = 449$ kOe at 275 K, with an error of 1 kOe. The B-site hyperfine field remains approximately constant with Al substitution, while for the A site a slight decrease with increasing Al content was observed.

Key Words—Al-Maghemite, Center shift, Maghemite, Mössbauer effect.

INTRODUCTION

Maghemite is a cation deficient spinel with 21 and $\frac{1}{3}$ Fe(III) ions distributed among eight tetrahedral (A) and sixteen octahedral (B) sites of the unit cell; 2 and $\frac{2}{3}$ sites per unit cell are vacant. It is commonly represented by the formula $(\text{Fe})[\text{Fe}_{5/3}\square_{1/3}]\text{O}_4$, where () denotes tetrahedral sites, [] octahedral sites and \square vacancies. However, some authors also report the vacancies to enter both octahedral and tetrahedral sites simultaneously (Armstrong *et al.*, 1966; Annersten and Hafner, 1973; Haneda and Morrish, 1977). Besides its technological importance as a material for recording devices, maghemite is of considerable geophysical interest since it occurs in many tropical magnetic soils (Schwertmann and Fechter, 1984; Fontes and Weed, 1991) and is believed to be a significant constituent of the Martian surface (Coey *et al.*, 1990).

The magnetically split Mössbauer spectrum of maghemite is composed of two sextets, hardly distinguishable at room temperature (RT) due to the fact that the hyperfine parameters for the two sites are very similar in magnitude. Commonly occurring effects such as small-particle size distributions and partial substitution of the iron atom by another cation tend to cause line broadening and/or a line-shape asymmetry, and in many cases the RT spectrum has to be fit with a distribution of unresolved A- and B-site hyperfine fields

(de Bakker *et al.*, 1991). On lowering the temperature it is possible, depending on the crystallinity, to obtain a somewhat better resolution of the two sites, but the only way to have them sufficiently separated is by applying strong external magnetic fields (Armstrong *et al.*, 1966).

In surveying the literature for maghemite it was noticed that an inconceivably wide scatter for the quoted center shifts (δ) exists, with values at RT ranging from 0.04 mm/s up to 0.30 mm/s for the A-site (δ_{A}) and from 0.04 mm/s up to 0.40 mm/s for B-site (δ_{B}), all relative to metallic iron. At 4.2 K values as high as 0.48 mm/s for δ_{A} and 0.62 for δ_{B} have been reported (Pollard, 1988; Pollard and Morrish, 1987; Collyer *et al.*, 1988; Mehner *et al.*, 1990; de Bakker *et al.*, 1991; Nikumbh *et al.*, 1992). In an attempt to resolve this discrepancy, variable-temperature Mössbauer spectra (MS) between 8 K and 475 K, and in addition at 4.2 K and 275 K with the absorber subjected to an external field of 60 kOe, were collected for a number of well-crystallized maghemite and Al-maghemite samples. The spectra have been interpreted using different approaches.

EXPERIMENTAL PROCEDURES

Al-maghemite samples were prepared by Bryan (1993) as follows: approximately 1 g of synthetic Al-

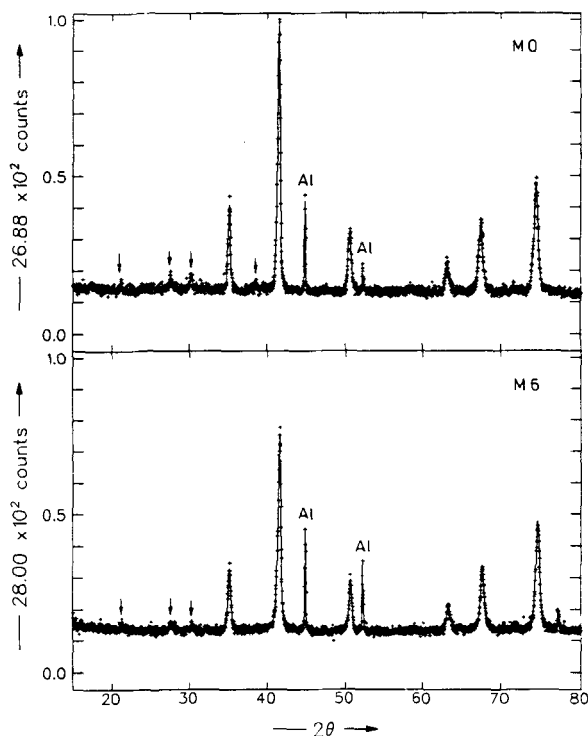


Figure 1. X-ray diffraction pattern of samples M0 and M6. Some superstructure lines due to the ordered arrangement of vacancies on the octahedral sites of the spinel lattice are indicated by arrows. Peaks at 44.8° and 52.3° (2θ) are due to the sample holder.

hematite was added to an aqueous solution of sucrose in such a way that a weight proportion of 1:4 (hematite/sucrose) was obtained. Maximum mixing was obtained by dispersion using a Sonifer, Cell Disrupter W-350 (Branson Sonic Power Co.), for approximately one minute. Afterwards the mixtures were immediately quick frozen, followed by freeze drying. The dried mixtures were then heated at 450°C for 30 minutes, followed by cooling, grinding, milling and reheating at 250°C . The samples are henceforward named as MX ($M = 0, 3, 6, 8, 11$ and 15 ; $X = 100y$), where y stands for the aluminum content in $\gamma\text{-(Al,Fe}_{1-y}\text{)}_2\text{O}_3$.

Powder X-ray diffraction patterns (XRD) were obtained using a Philips diffractometer with $\text{CoK}\alpha$ radiation and a graphite monochromator. The scans were done in the range of 15° – 80° (2θ) at a speed of $\frac{1}{4}^\circ \text{min}^{-1}$, and the reflected intensities were recorded in 1024 channels of a multichannel analyser. The numerical patterns were fitted with a sum of pseudo-Lorentzian peak shape functions, two for each reflection in order to account for the $\text{K}\alpha_1$ and $\text{K}\alpha_2$ radiation. Mean crystallite diameters (MCD) were estimated from the full widths at half maximum (FWHM) using Scherrer's equation with $K = 0.9$. The instrumental contribution to the peak width was evaluated from the diffractogram

of a well-crystallized commercial hematite sample, annealed at 1000°C in oxygen atmosphere for 24 hours. Lattice parameters were determined by the Nelson-Riley extrapolation method (Klug and Alexander, 1974).

Mössbauer spectra of all synthetic samples were collected at a temperature of 8.0 K and between 80–475 K at steps of 25 K. A time-mode spectrometer with a constant-acceleration drive and a triangular reference signal was used. The temperature stability of the absorber in the flow-cryostat/furnace combination was better than 0.5 K. All absorbers were prepared by mixing an amount of material with very pure carbon in order to achieve a homogeneous thickness of approximately 10 mg Fe/cm^2 . The spectrometer was periodically calibrated using the spectrum of a well-crystallized hematite, prepared after heating a commercial hematite sample (Merck) at 1000°C in oxygen atmosphere for 24 hours. External field (H_{ext}) of 60 kOe ($\text{Oersted} = \text{cm}^{-1/2} \cdot \text{g}^{1/2} \cdot \text{s}^{-1}$) parallel to the direction of the incident γ -rays was applied at 4.2 K and 275 K. For these measurements the calibration spectra were recorded simultaneously using another source and counting electronics at the opposite end of the transducer. Center shifts are quoted relative to metallic iron. Details about the fitting procedures are given below.

RESULTS AND DISCUSSION

Figure 1 shows the XRD patterns for synthetic samples M0 and M6. All observed peaks can be assigned to the spinel phase. Some superstructure lines are clearly visible, indicating an ordered arrangement of the vacancies on the B sites (Haneda and Morrish, 1977). The diffractograms for the other samples all resemble those shown in Figure 1. Mean crystallite diameter values along the (220) and (311) lattice directions are 44 and 35 nm for M0, 39 and 41 nm for M6 and 26 and 23 nm for M15 samples. The ordered arrangement of vacancies seems to be related to the MCD values since for samples of particle size less than 20 nm the superstructure lines are not observed (Haneda and Morrish, 1993). The lattice parameters are 0.8354 nm for M0, 0.8327 nm for M6 and 0.8321 for M15 samples, with an estimated error of 0.0005 nm. The value for the non-substituted maghemite sample is somewhat larger than expected due to the presence of a small amount of magnetite in the sample (see Mössbauer results below). More structural and thermal details for the various samples can be found elsewhere (Bryan, 1993; Bowen *et al.*, 1994).

In the range of temperatures between 80 K and 475 K all zero-field MS consist of a magnetically split sextet and a weak doublet (usually less than 2%). This latter component was fitted as a symmetric doublet with all parameters fixed at: $\Delta E_Q = 0.60 \text{ mm/s}$; $\delta = 0.36 \text{ mm/s}$ and $\Gamma = 0.35 \text{ mm/s}$, ΔE_Q and Γ being the quadrupole splitting and line width (FWHM) respectively. These

values were chosen on the basis of several trial fits to a few selected spectra. This doublet is not due to any impurity in the counter or in the cryostat windows, but, considering its low intensity and the apparent lack of any effect of its Mössbauer parameters on those for the maghemite component, no further attention was paid to its origin. The magnetic components could be fitted with a superposition of two Lorentzian-shaped, symmetrical sextets, but two different converging models appears to be applicable, both leading to similar goodness-of-fit (χ^2) values. In all cases the following parameter constraints were used: quadrupole shift $\epsilon_Q = 0$ fixed for both sites; three width parameters, equal for both subspectra; line-area ratios fixed at 3:2:1 and also fixed B- to A-site area ratio of 62.5:37.5, i.e., assuming random Al distribution and vacancies in octahedral sites only. Allowing the quadrupole shifts to vary did not improve the fits significantly.

A typical experimental spectrum (M6 at 8 K) is shown in Figure 2a, together with the fitted subspectra and their superposition (full lines). This fit, in which the first line (i.e., left-most absorption) of the B-site component is at higher absolute velocity than the first line of the A-site component, will be called Model 1. Some relevant parameters for M6, as obtained from this model, are given in Table 1 for a few selected temperatures. The other samples exhibit very similar results, with the hyperfine fields and center shifts showing slight variations with the Al substitution.

As seen from Table 1, Model 1 yields a nearly constant difference $\Delta H_{hf} = H_{hf,B} - H_{hf,A}$ of approximately 15 kOe, increasing somewhat when the temperature is raised to 475 K. In contrast, the difference $\Delta\delta = \delta_B - \delta_A$ is 0.10 mm/s at 8 K, 0.04 mm/s at 275 K, and -0.06 mm/s at 475 K, i.e., at a certain temperature in the vicinity of room temperature, δ_A seems to become larger than δ_B . This latter phenomenon is totally unexpected and hard to understand because the cation-oxygen bond-length is less for A sites than for B sites and hence the center shift at any temperature is expected to be larger for the octahedral ions (Armstrong *et al.*, 1966), as is commonly observed for spinel ferrites (Vandenberghe and De Grave, 1989). Moreover, the apparently large temperature variation of δ_A cannot be explained by any reasonable value for the characteristic Mössbauer temperature determining the second-order Doppler shift in terms of the Debye model for the lattice vibrations (De Grave and Van Alboom, 1991).

Depending on the initial values of the adjustable parameters, the fitting routine was often found to converge to a solution in which the first line of the B-site component is at lower absolute velocity than the first line of the A-site component, as shown in Figure 2b. This type of fit will hereafter be referred to as Model 2. The as-such obtained χ^2 is, in many cases, somewhat smaller as compared to the values calculated from

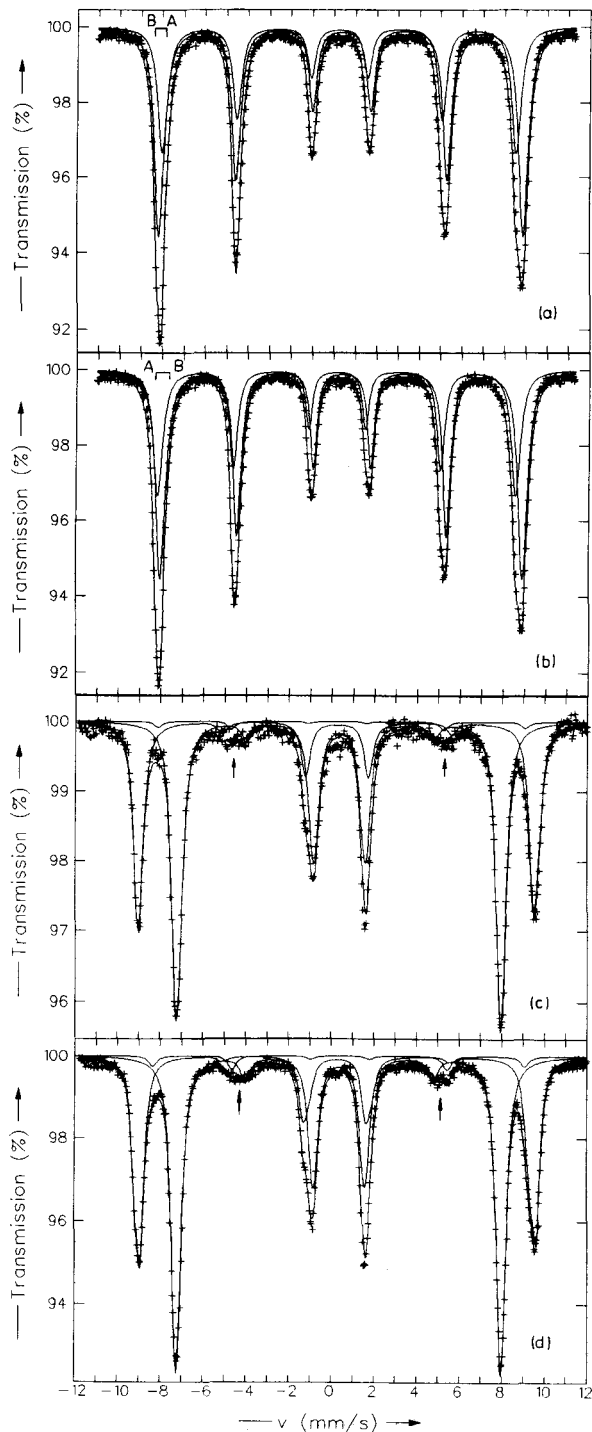


Figure 2. Mössbauer spectra of some selected samples: a) M6 at 8 K fitted with Model 1; b) M6 at 8 K fitted with Model 2; c) M0 at 4.2 K and applied field of 60 kOe; d) M6 at 4.2 K and applied field of 60 kOe. Crosses represent the experimental data, and full lines represent the calculated subspectra and their sum. The position of the first lines of A and B sites is indicated in Figures 2a and 2b. The arrows in Figures 2c and 2d show the position of lines 2 and 5.

Table 1. Hyperfine fields $H_{\text{hf,B}}$, $H_{\text{hf,A}}$ and their differences ΔH_{hf} in kOe and center shifts δ_{B} , δ_{A} and their differences $\Delta\delta$ in mm/s obtained from fitting the spectra of sample M6 with Model 1 and Model 2. The estimated statistical errors are 2 kOe for H_{hf} and 0.02 mm/s for δ .

Temp. (K)	$H_{\text{hf,B}}$	$H_{\text{hf,A}}$	ΔH_{hf}	δ_{B}	δ_{A}	$\Delta\delta$
Model 1						
8	528	514	14	0.47	0.37	0.10
80	527	511	16	0.46	0.37	0.09
275	504	489	15	0.37	0.33	0.04
475	456	436	20	0.19	0.25	-0.06
Model 2						
8	525	519	6	0.52	0.29	0.23
80	524	518	7	0.51	0.28	0.23
275	499	497	2	0.43	0.22	0.21
475	448	452	-4	0.29	0.07	0.22

Model 1, but not appreciably so, making it difficult to judge which fit model is to be preferred as far as reproducing the experimental line shape is concerned. The parameters for sample M6 as obtained from Model 2 are also listed in Table 1.

As can be seen from Figures 2a and 2b both models describe the experimental spectra in an equally adequate way. Furthermore, each of the two adjusted parameter sets are in accordance with some of the literature data, although considerable differences between the hyperfine parameters are obtained by the two models. Some representative center-shift and hyperfine-field data for maghemites at room temperature and 4.2 K as quoted in the literature are listed in Table 2. There is clearly a wide scatter in these values, and although some authors did not specifically show the calculated subspectra in their papers, it is believed that this scatter is related to the two possible models of fitting as re-

ported in the present paper. It should be stressed at this point that convergence to any of the two models seems to be totally arbitrary in the sense that the output results are determined by the input parameter values. It was necessary to try several different input-parameter sets in order to arrive at the iterated data as reported in Table 1, because no straightforward correlation between the input parameters and the resulting fit could be established.

In an attempt to reconcile the apparent discrepancies concerning the maghemite hyperfine parameters, external-field measurements (60 kOe) at 4.2 K for all samples and at 275 K (this was the highest temperature which could be applied with the available system) for samples M0 and M6 have been performed. With such a strong field it was possible to separate the two sites, allowing the determination of the hyperfine parameters with a relatively high precision. The spectra were fitted with two main asymmetric sextet components. The asymmetry is due to the combined effects of random orientation of the hyperfine field with respect to the electric-field-gradient's principal axis and a non-zero dipolar contribution to the hyperfine field (De Grave *et al.*, 1993). For all maghemites at 4.2 K a small hematite fraction (less than 3 mole %) could be detected in the external-field spectra (Bowen *et al.*, 1994). The M0 spectra at 275 K, both with and without the external field, show that this sample in addition contains approximately 4 mole % of a magnetite impurity. This magnetite component was included in the fits, its hyperfine parameters being fixed at their respective values recently found by De Grave *et al.* (1993) for pure magnetite.

Some representative experimental and calculated spectra are shown in Figures 2c and 2d, and relevant evaluated parameters are listed in Table 3. Some of

Table 2. Center shifts (relative to metallic iron, in mm/s) and hyperfine fields (kOe) for non-substituted maghemite as reported in literature. For the external-field results, $H_{\text{hf,A}}$ and $H_{\text{hf,B}}$ are the effective hyperfine fields (see text).

Temp.	δ_{B}	δ_{A}	$\Delta\delta$	$H_{\text{hf,A}}$	$H_{\text{hf,B}}$	Ref.	Comments
RT	0.40	0.20	0.20	497.2	497.3	1	model 2
	0.35	0.24	0.11	504.9	474.0	1	$H_{\text{ext}} = 16$ kOe
	0.04	0.04	0.00	493	507	2	*
	0.324	0.304	0.020	488	501	3	
	0.31	0.23	0.08	494.1	496.3	4	model 2
4.2 K	0.47	0.41	0.06	480.0	515	5	
	0.46	0.42	0.04	520.4	521.0	1	
	0.50	0.36	0.14	570.9	469.8	1	$H_{\text{ext}} = 61$ kOe
	0.62	0.48	0.14	562	482	6	$H_{\text{ext}} = 50$ kOe Co: γ -Fe ₂ O ₃
	0.487	0.356	0.131	554	491	3	$H_{\text{ext}} = 42$ kOe

¹ Pollard (1988).

² Mehner *et al.* (1990).

³ Collyer *et al.* (1988).

⁴ Nikumbh *et al.* (1992).

⁵ de Bakker *et al.* (1991).

⁶ Pollard and Morrish (1987).

* The authors did not mention if the quoted values are relative to the source or to metallic iron.

Table 3. Hyperfine fields (kOe), center shifts (mm/s) and canting angles θ ($^\circ$) of samples M0, M3, M6, M8, M11 and M15 derived from the 60 kOe applied-field measurements at 4.2 K. Samples M0 and M6 were measured at 275 K as well. The errors are 1 kOe for H_{eff} , 4 kOe for H_{hf} , and 0.005 mm/s for δ .

Sample	T (K)	$H_{\text{eff,B}}$	$H_{\text{eff,A}}$	θ_B	θ_A	$H_{\text{hf,B}}$	$H_{\text{hf,A}}$	ΔH_{hf}	δ_B	δ_A	$\Delta\delta$
M0	4.2	471	575	165	17	529	518	11	0.491	0.370	0.121
	275	449	562	166	20	507	506	1	0.357	0.233	0.124
M3	4.2	472	575	162	17	529	517	12	0.486	0.371	0.115
M6	4.2	471	574	162	13	529	515	14	0.481	0.369	0.112
	275	444	557	167	17	504	500	4	0.348	0.218	0.130
M8	4.2	472	572	161	13	529	514	15	0.481	0.365	0.116
M11	4.2	471	572	162	12	529	514	15	0.478	0.365	0.113
M15	4.2	471	571	162	13	529	513	16	0.476	0.360	0.116

these data have been reported briefly in an earlier paper (Bowen *et al.*, 1994), but are repeated here for the ease of the discussion. From Table 3 it can be seen that the B-site effective hyperfine field, $H_{\text{eff,B}}$, at 4.2 K remains approximately constant with Al substitution, while for the A-sites a slight decrease with increasing Al content is found. As argued by Bowen *et al.*, this variation (or lack of variation in the case of B-site ferric ions) is consistent with the Al ions occupying the B sites exclusively. Both δ_A and δ_B seem to decrease with increasing Al concentration. The variations are weak, but believed to be significant. An explanation for it has not been found yet. Finally, the solubility limit for the Al species in the maghemite structure, as reported earlier by Wolska and Schwertmann (1989) to be 10 at %, could not be confirmed.

Another important feature of the in-field spectra for the maghemite components is the presence of lines 2 and 5. These absorptions are expected to be absent if the hyperfine fields are completely aligned along the external field. From the relative areas $A_{1,6}/A_{2,5}$ one can determine the canting angle θ , defined as the angle between \vec{H}_{hf} and \vec{H}_{ext} (Vandenberghe and De Grave, 1989). On the other hand, the measured effective hyperfine fields are given in the following, well-known equation:

$$H_{\text{eff}}^2 = H_{\text{hf}}^2 + H_{\text{ext}}^2 - 2H_{\text{ext}}H_{\text{hf}}\cos(\pi - \theta).$$

Thus, knowing the area ratios $A_{1,6}/A_{2,5}$ one can calculate θ and H_{hf} . Since the A- and B-site components are well separated in the external-field spectra, the adjusted H_{eff} values are not affected by the various restrictions imposed to the fit procedure. On the other hand, the adjusted values for the spectral areas of lines 2 and 5 were observed to be dependent to some extent on the imposed fitting conditions, so that the canting angles θ , and hence the hyperfine fields, cannot be determined with very high precision. For the present experiments, an uncertainty of about 4 kOe for the H_{hf} values given in Table 3 is estimated based on the results of numerous trial fits. In a recent paper of de Jesus Filho *et al.* (1993) it was proposed that in Al-substituted maghemites, comparable to the samples used in

this study, the A-site moments are completely aligned with H_{ext} , while those from the B sites are canted by about 30° . However, no details about the applied fitting procedures were indicated by the authors. The present results disagree with that conclusion. According to the data of Table 3, which refer to the best fits for any of the given samples, the sum $\theta_A + \theta_B$ is close to 180° regardless of the Al substitution, meaning that within experimental and statistical uncertainties the A- and B-site magnetic moments are collinear for all involved maghemites.

In summary, the results listed in Table 3 for the synthetic maghemites clearly show that the hyperfine parameters obtained from fitting the zero-field MS with Model 2 are in serious discrepancy with the more reliable and acceptable external-field results, in particular as far as the difference of about 0.20 mm/s between the B- and A-site center shifts is concerned. This discrepancy persists even in the data referring to 8 K. On the other hand Model 1 gives acceptable results at low temperatures, but cannot be used to fit high-temperature measurements. For both models the disagreements are more significant for the A-site, probably due to the lower intensity of this component. An important general conclusion that can be drawn from these results is that the application of an external magnetic field is absolutely essential if one wants to extract reliable information from the Mössbauer spectra of maghemites. As external-field spectrometers are not routinely accessible for the vast majority of the Mössbauer labs, an alternative way to derive acceptable parameter values from zero-field spectra might be to keep the difference between δ_B and δ_A fixed in fitting the spectra. This procedure will be tested systematically by future work in this laboratory on other synthetic, and also on various environmental maghemite systems. The principal question in that respect is whether the value of 0.12 ± 0.01 mm/s for this difference in center shifts is unique or whether it changes depending on the morphology and composition of the samples.

At this stage, an important finding in favour to the above suggested procedure should be mentioned. It concerns the results obtained for the maghemite phase

present in some Brazilian soils, in which the difference between the B- and A-site center shifts were also found to be close to 0.12 mm/s.

CONCLUSIONS

The Mössbauer parameters extracted from the external-field spectra are beyond any doubt the most precise that can be obtained for synthetic and natural maghemites and substituted-maghemites. The wide scatter existing for center-shift and hyperfine-field literature data as obtained from zero-field spectra, is concluded to be an artifact of the fit procedures. Using a 60 kOe applied-field it was determined that the center shifts for the A- and B-sites are different by a constant amount of 0.12 mm/s on the average, at least for the range of temperatures between 4.2 K–275 K. Slight variations of some of the hyperfine parameters with the Al content have been observed for the synthetic Al maghemites.

ACKNOWLEDGMENTS

This work was supported in part by the Fund for Joint Basic Research (Belgium), by a NATO collaborative Research Grant 91/0116 and by CNPq (Brazil). The authors wish to thank A. M. Bryan (North Carolina State University) for the sample preparations.

REFERENCES

- Annersten, H. and Hafner, S. S. (1973) Vacancy distribution in synthetic spinels of the series Fe_3O_4 - γ - Fe_2O_3 : *Z. Kristallog.* **137**: 321–340.
- Armstrong, J. R., Morrish, A. H., and Sawatzky, G. A. (1966) Mössbauer study of ferric ions in the tetrahedral and octahedral sites of a spinel: *Phys. Lett.* **23**: 414–416.
- Bowen, L. H., De Grave, E., and Bryan, A. M. (1994) Mössbauer studies in external field of well crystallized Al-maghemites made from hematite: to be published in *Hyperfine Interactions*.
- Bryan, A. M. (1993) The thermal transformation of Al-substituted hematite and lepidocrocite to maghemite studied by ^{57}Fe Mössbauer spectroscopy: Ph.D. thesis, North Carolina State University, USA.
- Coey, J. M. D., Mørup, S., Madsen, M. B., and Knudsen, J. M. (1990) Titanomaghemite in magnetic soils on earth and Mars: *J. Geophys. Res.* **95**: 14.423–14.425.
- Collyer, S., Grimes, N. W., Vaughan, D. J., and Longworth, G. (1988) Studies of the crystal structure and crystal chemistry of titanomaghemite: *Amer. Mineral.* **73**: 153–160.
- de Bakker, P. M. A., De Grave, E., Vandenberghe, R. E., Bowen, L. H., Pollard, R. J., and Persoons, R. M. (1991) Mössbauer study of the thermal decomposition of lepidocrocite and characterisation of the decomposition products: *Phys. Chem. Minerals* **18**: 131–143.
- De Grave, E. and Van Alboom, A. (1991) Evaluation of ferrous and ferric Mössbauer fractions: *Phys. Chem. Minerals* **18**: 337–342.
- De Grave, E., de Bakker, P. M. A., Bowen, L. H., and Vandenberghe, R. E. (1992) Effect of crystallinity and Al substitution on the applied-field Mössbauer spectra of iron oxides and oxyhydroxides: *Z. Pflanzenernähr. Bodenk.* **155**: 467–472.
- De Grave, E., Persoons, R. M., Vandenberghe, R. E., and de Bakker, P. M. A. (1993) Mössbauer study of the high temperature phase of Co-substituted magnetites, $\text{Co}_x\text{Fe}_{3-x}\text{O}_4$. I. $x \leq 0.04$: *Phys. Rev. B* **47**: 5881–5893.
- de Jesus Filho, M. F., da Nova Mussel, W., Qi, Q., and Coey, J. M. D. (1993) Magnetic properties of aluminum-doped $\gamma\text{Fe}_2\text{O}_3$: Proc. 6th Int. Conf. on Ferrites, Tokyo 1992 (in press).
- Ericsson, T., Krisnhamarthy, A., and Srivastava, B. K. (1986) Morin transition in Ti-substituted hematite: A Mössbauer study: *Phys. Scripta* **33**: 88–90.
- Fontes, M. P. F. and Weed, S. B. (1991) Iron oxides in selected Brazilian Oxisols: I. Mineralogy: *Soil Sci. Soc. Am. J.* **55**: 1143–1149.
- Haneda, K. and Morrish, A. H. (1977) Vacancy ordering in $\gamma\text{-Fe}_2\text{O}_3$ small particles: *Solid State Commun.* **22**: 779–782.
- Haneda, K. and Morrish, A. H. (1993) Structural peculiarities in magnetic small particles: *Nuclear Instruments and Methods in Physics Research B* **76**: 132–137.
- Klug, H. P. and Alexander, L. E. (1974) *X-ray Diffraction Procedures for Polycrystalline and Amorphous Materials*: John Wiley and Sons, New York.
- Mehner, H., Koppe, H. J., and Mörke, W. (1990) Mössbauer investigation of $\gamma\text{-Fe}_2\text{O}_3$ particles: *Hyperfine Interactions* **54**: 609–612.
- Nikumbe, A. H., Aware, A. D., and Sayanekar, P. L. (1992) Electrical and magnetic properties of $\gamma\text{-Fe}_2\text{O}_3$ synthesized from ferrous tartarate one and half hydrate: *J. Magn. Mater.* **114**: 27–34.
- Pollard, R. J. (1988) On the Mössbauer spectrum of $\gamma\text{-Fe}_2\text{O}_3$: *Hyperfine Interactions* **41**: 509–512.
- Pollard, R. J. and Morrish, A. H. (1987) High-field magnetism in non-polar $\gamma\text{-Fe}_2\text{O}_3$ recording particles: *IEEE Trans. Magn.* **MAG(23)**: 42–44.
- Schwertmann, U. and Fechter, H. (1984) The influence of aluminum on iron oxides: XI. Aluminum-substituted maghemite in soils and its formation: *Soil Sci. Soc. Am. J.* **48**: 1462–1463.
- Vandenberghe, R. E. and De Grave, E. (1989) Mössbauer effect studies of oxidic spinels: in *Mössbauer Spectroscopy Applied to Inorganic Chemistry*, Vol. 3, G. J. Long and F. Grandjean, eds., Plenum, New York, 59–182.
- Wolska, E. and Schwertmann, U. (1989) The vacancy ordering and distribution of aluminium ions in $\gamma\text{-(Fe,Al)}_2\text{O}_3$: *Solid State Ionics* **32/33**: 214–218.

(Received 14 July 1993; accepted 11 March 1994; Ms. 2404)